Continuous Degeneracy and Magnetization Process in the 3D FCC Kagome Lattice with the Dipole-Dipole Interaction

by

©Andrew Way

A thesis submitted to the School of Graduate Studies in partial fulfillment of the requirements for the degree of

Bachelor of Science

Department of Physics

Memorial University of Newfoundland

May 2017

St. John's Newfoundland

Abstract

Results are presented on analytic and computational analyses of the spin states associated with ABC stacked kagome planes of magnetic ions with only long-range dipole-dipole interactions. Extending previous work on the 2D kagome system, where six-fold discrete degeneracy of the ground state was revealed [1], we show that the 3D FCC kagome lattice exhibits a continuous degeneracy characterized by just six sub-lattice spin vectors and two spherical angles. Thermal fluctuations are shown to lift this degeneracy in an order-by-disorder process. Degaussing the lattice with a magnetic field applied along directions of high symmetry also results in lifting the continuous degeneracy to a subset of states from the original set of ground states, characterized by a single parameter. This lattice type is a model for the magnetic Mn ions in IrMn3, the most popular compound used as the antiferromagnetic pinning layer in hard-drive spin valve structures [2]. Analysis of these spin states is relevant for a deeper understanding of magnetic and thermal stability at surfaces and in thin films of IrMn3.

Acknowledgements

At a minimum you must acknowledge the funding sources for your work.

Table of Contents

List of Tables

List of Figures

List of Abbreviations and Symbols

If you don't have a list of abbreviations, then you don't need to include this file and you can comment out the corresponding lines in your main .tex file. For example, if this file just defined a couple of terms such as AFM, then you wouldn't necessarily need this.

If you do have abbreviations to define, then you will probably set them up in a table like this:

E	energy
$\vec{E}$	electric field
EFMS	Erika

Chapter 1

Introduction (can be a more descriptive title)

1.1 A section

Your first step in using this template should be to rename the folder and main .tex file to something involving your name. That will help me to keep track of the various theses I'm reading!

1.1.1 A subsection about getting organized

Then start creating an outline for your thesis. If you already have chapters written as papers, perhaps you should be using the "MUN_Thesis_multiple_bibliographies" template.

To create the outline, create the chapters and write in all of the sections, subsections, etc. Then send that file to me so that I can look it over. This is particularly important for the introduction or background chapter. If we agree on the scope of your thesis up front, you will save yourself time later.

1.1.2 Scope

The main purpose of the first section is to provide the context for your work. What have other people done in this area, with these techniques? What background information does a somewhat general reader (*e.g.* chemist just starting a graduate program) need to know in order to appreciate and understand your work?

1.2 Another section

As you write your thesis, be sure to use labels and references for your tables, figures, equations, chapters, etc. This is another important aspect of getting organized, a topic which was discussed in Section 1.1.1. Be sure to pick unique labels. For example, “raman” or "afm" are probably not good labels, since you will probably have multiple figures, tables, equations, and sections which could carry those labels. Your whole thesis, including material in, for example, Appendix A, will have one common list of labels.

Note the pretty quotes around raman and the not-so-pretty quotes around afm. See the .tex file to know how to do this.

1.2.1 Some technical details

Pretty much all equations should be set off and numbered rather than included inline. The Tabor coefficient, μ, can be used to determine whether material deformation should be taken into account. [**?**]

$$\mu = \left[\frac{R(\Delta\gamma)^2}{E^{*2}\sigma^3}\right]^{1/3} \tag{1.1}$$

where R is the indenter tip radius, $\Delta\gamma$ is the work of adhesion, σ is the separation, and E^* is defined as

$$\frac{1}{E^*} = \frac{1-\nu_{\text{tip}}^2}{E_{\text{tip}}} + \frac{1-\nu_{\text{sample}}^2}{E_{\text{sample}}} \tag{1.2}$$

ν_{tip} is....

Note that the equations are part of a paragraph. Check how this is done in the .tex file, by not leaving blank lines before or after the equation. Also, note that the font used in the text for the symbols is the same as that used in the equation, and that text in the equation doesn't need to be in math mode.

Chapter 2

Methods

2.1 Substrate preparation

This is a good chapter to write continuously throughout your degree program. It will be easier to write up a procedure while it's fresh in your mind, and that way you won't be hunting down an instrument model or consumables supplier later.

If you are varying several parameters in your procedure, you may want to tabulate your different combinations. Table 2.1 summarizes ice cream texture characteristics used by McGhee et al [**?**].

Table 2.1: Note how this caption is at the top of the table. Also, note that the caption in the List of Tables doesn't include the reference number. [**?**].

Characteristic	Mean value
Icy	4.63
Crumbly	4.75
Fluffy	4.58
Gummy	4.71
Sandy	4.58
Soggy	4.29
Weak body	3.92

2.1.1 Lots of chemicals

I used K_2HPO_4, $KH_2PO_4 \cdot 2\,H_2O$, and other salts containing PO_4^{3-} ions. Best of all, I didn't write out those chemical formula by hand using subscripts and superscripts. See the .tex file to find out how!

2.2 Atomic Force Microscopy

A picture is worth a thousand words! If you are creating your own schematics, consider using a program which will saves images in a precise and generally readable format such as SVG. Inkscape will do that for you and is open source.

There are many public domain and other freely reproducible images available on the Wikimedia Commons. You can also easily get permission to reuse a figure from most journals through RightsLink.

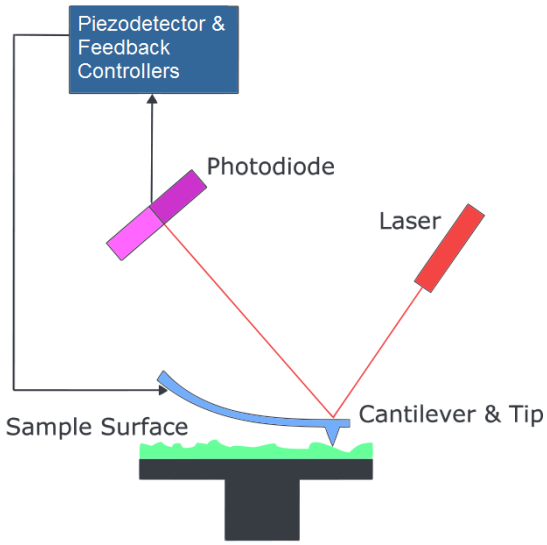

Figure 2.1: Schematic of an atomic force microscope. Note that the size of the text in the figure is comparable to the size of the main text. Reproduced under Public Domain from Wikimedia Commons

Chapter 3

Another chapter

3.1 Ground State Degeneracy

In this chapter results of simulations on the dipolar kagome lattice are presented. EFM simulations reveal a many-fold degenerate ground state allowing zero-temperature states comprising a six-sublattice structure; three of the sublattices contain spins that are the negatives of the spins on the remaining three sublattices. The spins alternate in direction along the [1,1,1] direction.

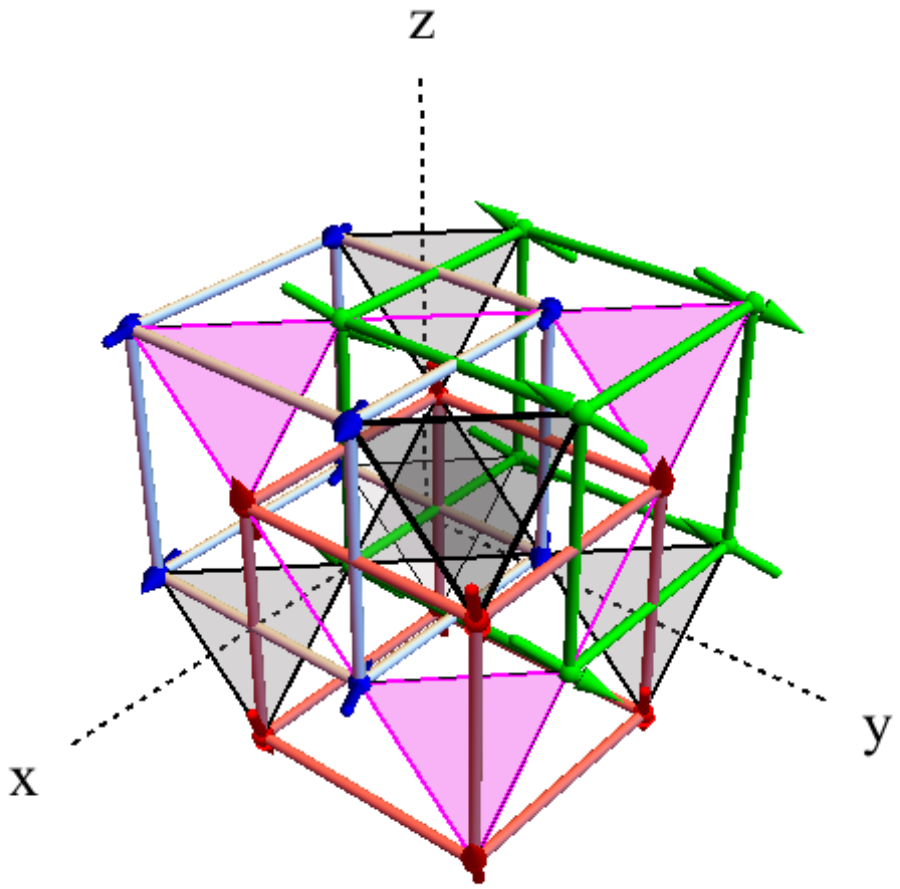

Figure 3.1: A view down the <1,1,1> axis of a 3D FCC lattice with six sub-lattice spin vectors.

Every ground state configuration obtained through the EFM simulation is characterized by the following set of equations:

$$\alpha = \sin\theta\cos\phi \tag{3.1}$$

$$\beta = \sin\theta\sin\phi \tag{3.2}$$

$$\chi = \cos\theta \tag{3.3}$$

$$\delta = (2a^2 - 1)/2c \tag{3.4}$$

$$\epsilon = \sqrt{(}1 - a^2 - d^2) \tag{3.5}$$

This set of equations acts as elementary building blocks for the components of the spin vectors that exist in the dipolar kagome ground state. There are two parameters that dictate the resulting ground state: θ and ϕ, which are polar angles of the spin "A". Spin A is arbitrarily chosen. The spin vectors themselves may be constructed as follows:

$$\overrightarrow{a} = (\alpha, \beta, \chi)$$

$$\overrightarrow{b} = (\delta, \epsilon, -\alpha)$$

$$\overrightarrow{c} = (-\epsilon, -\chi - \delta, \beta)$$

$$\overrightarrow{d} = -\overrightarrow{a}$$

$$\overrightarrow{e} = -\overrightarrow{b}$$

$$\overrightarrow{f} = -\overrightarrow{c}$$

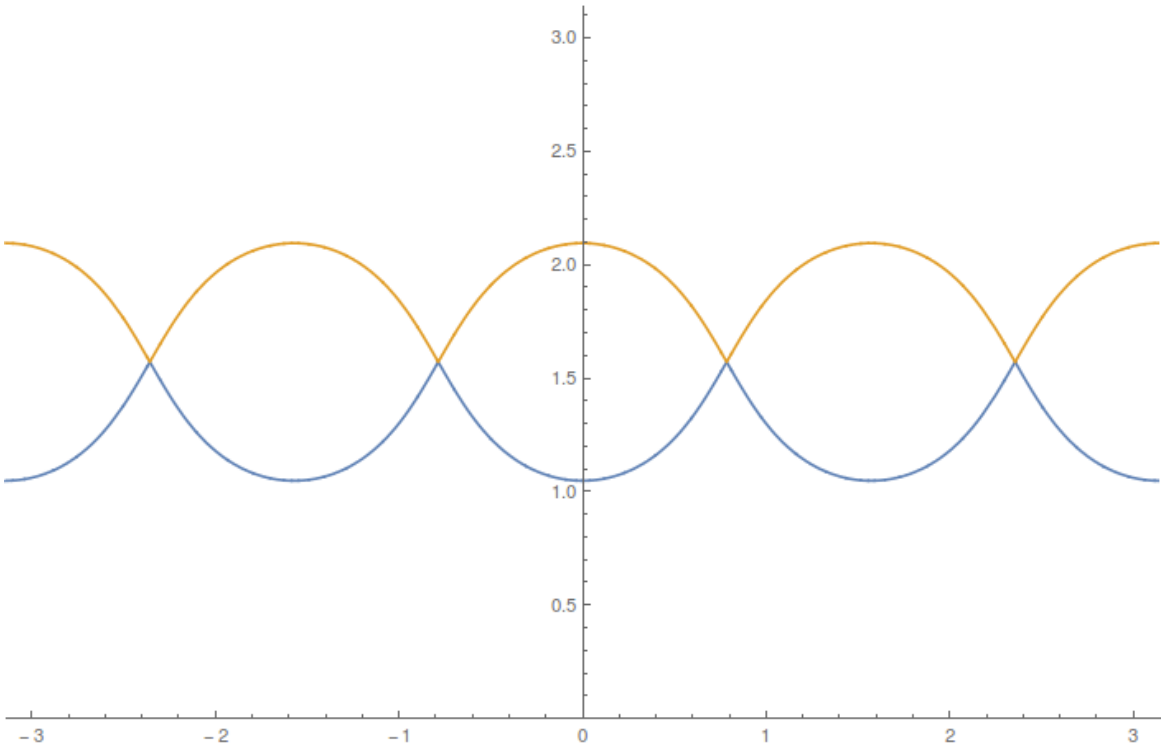

Figure 3.2: A plane that contains points that allow the construction of valid ground states.

Any theta and phi pair chosen from the plane in figure 3.2 will give rise to a valid ground state of the same energy with the exception of those pairs of theta and phi that lie within the bound region of the graph. Within the bound region of the graph, $e = \sqrt{(1-a^2-d^2)} \in \mathbb{C}$. At each node of each bound area, $d = (2a^2-1)/2c \rightarrow \pm 0/0$.

It is possible to reduce the size of this graph to 1/16 the size by showing that a state in each portion of the graph is relatable to an analogous state in the other portions of the graph via symmetry operations.

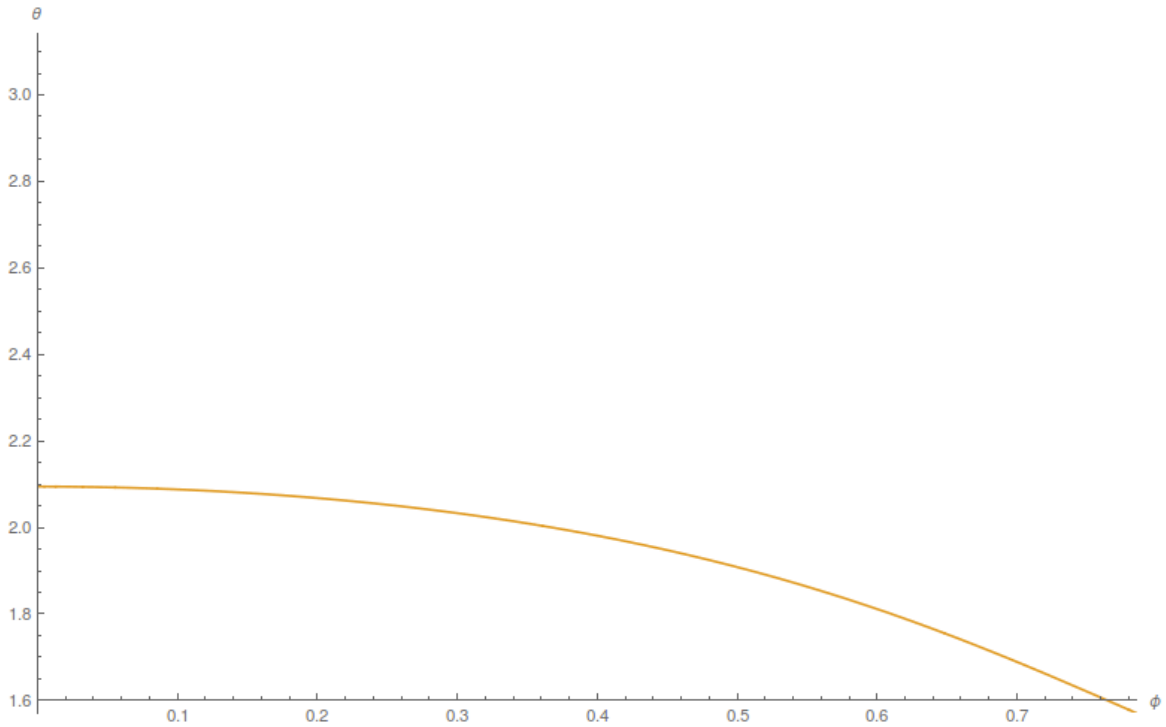

Figure 3.3: One section of the original degeneracy plane that is equivalent to all other sections of the plane due to symmetry operations.

3.1.1 Visualization of the Ground State

By generating the spin vectors described by equations 3.1,3.2,3.3,3.4, and 3.5, spin configurations ranging from planar to non-planar states can be obtained. An example of a non-planar state is shown in figure 3.4.

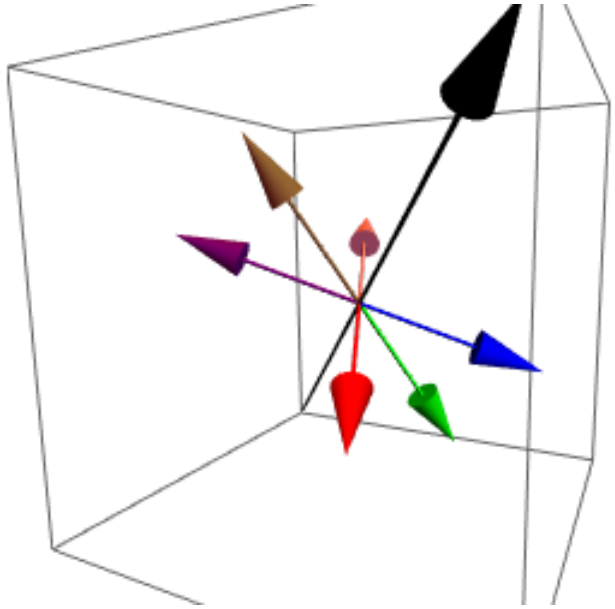

Figure 3.4: The six sublattice spins conjoined at their ends for clarity and illustration. The vector denoting <1,1,1> axis of symmetry is illustrated in black

To gain insight into what choices of θ and ϕ pairs give rise to particular states, consider the contour plot in fig. 3.5. The contour plot illustrates the volume of a parallelopiped formed by the a, b, and c spin vectors corresponding to a particular θ and ϕ chosen from fig. 3.3. It is from this illustration that one can obtain an understanding of what choices of θ and ϕ result in planar states or non-planar states.

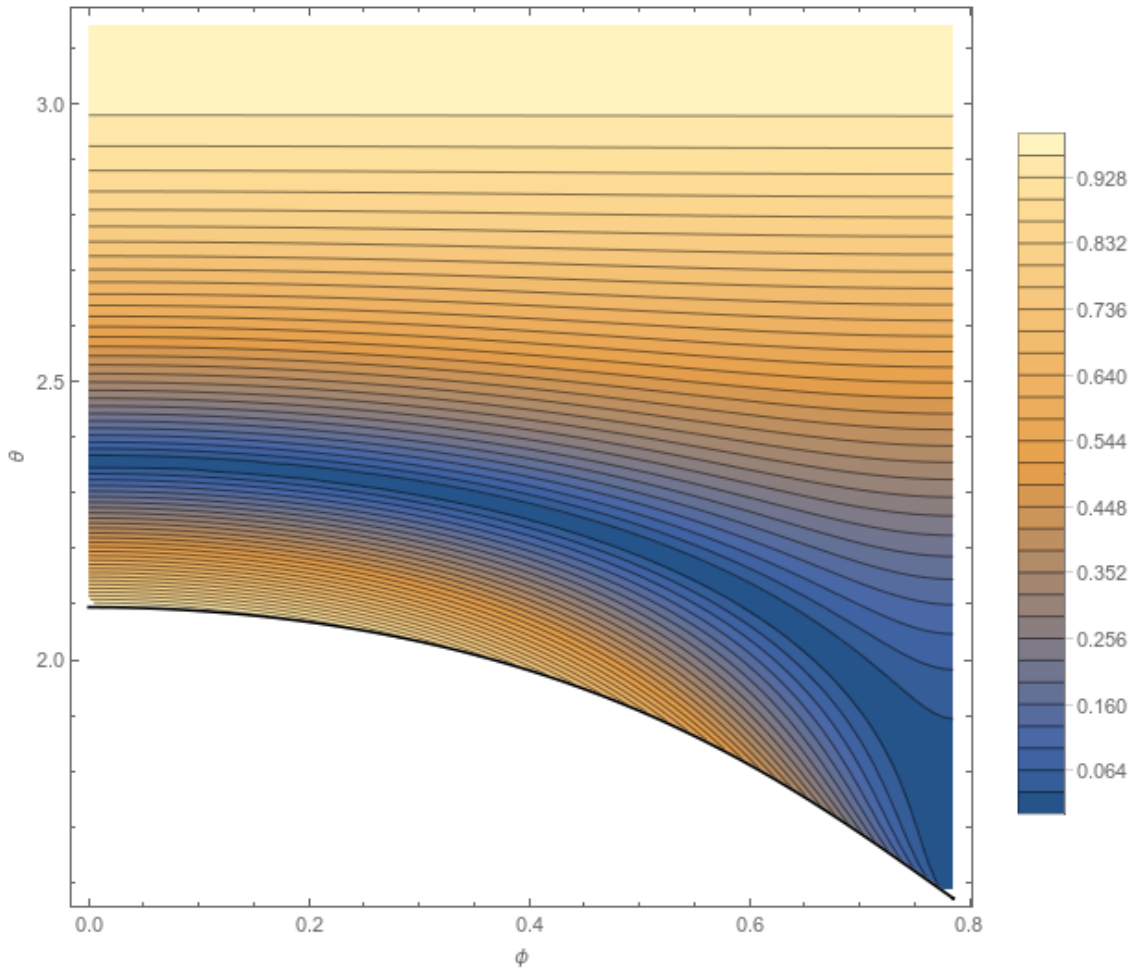

Figure 3.5: A contour plot of volume of a parallelopiped formed by a spin configuration with respect to θ and ϕ

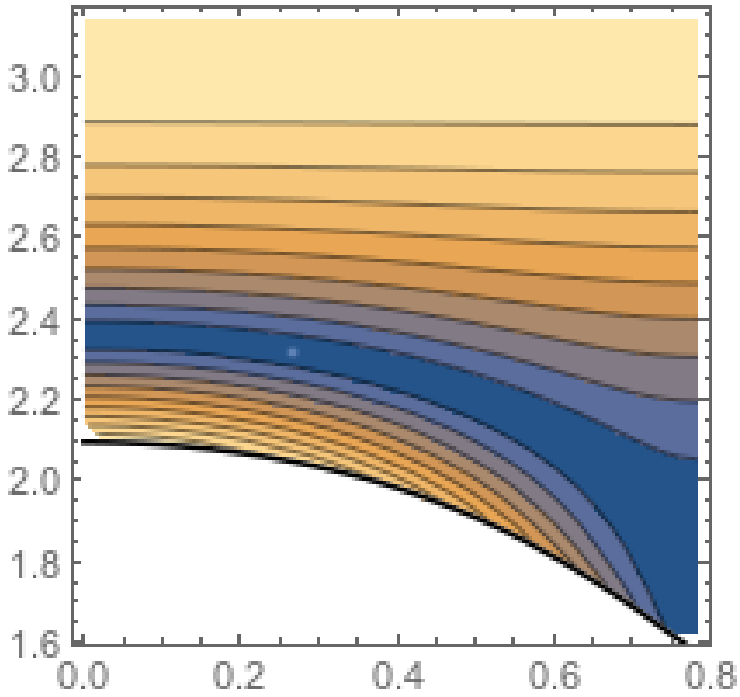

Figure 3.6: A contour plot of volume of a parallelepiped with respect to theta and phi. The point corresponding to theta=2.3108 and phi=0.27 is highlighted in green.

As an example, the point corresponding to a planar state located at the point θ=2.3108 and ϕ=0.27 was chosen, as shown in fig. 3.6.

Using equations (3.1),(3.2),(3.3),(3.4), and (3.5), the vectors were conjoined as shown in fig. 3.1.1.

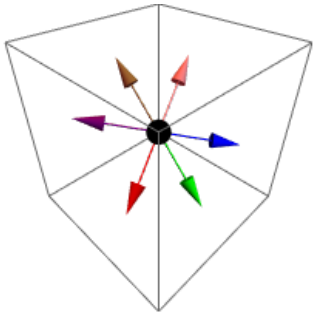

Figure 3.7: View 1

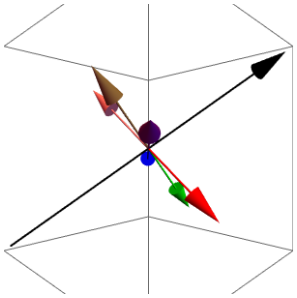

Figure 3.8: View 2

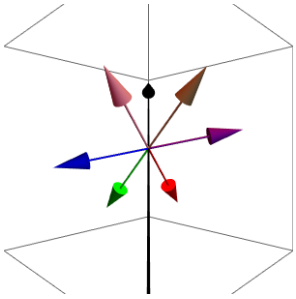

Figure 3.9: View 3

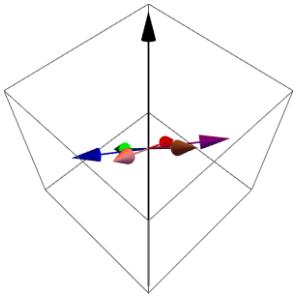

Figure 3.10: View 4

Figure 3.11: Four different perspectives of the same spin configuration corresponding to theta=2.3108 and phi=0.27

3.1.2 Planar Ground States

The thin strip of blue that cuts into the contour plot just above the complex region consists of the set of points that give rise to parallelopipeds with the smallest volume. This corresponds to spin configurations that are planar. Elsewhere in the plane, the spin configurations are non-planar. The strip of points that give rise to planar states are described by the following polar equations:

$$\phi = \frac{\pi}{4}\cos\gamma \tag{3.6}$$

$$\theta = \frac{\pi}{4}(\sin\gamma + 2) \tag{3.7}$$

The spin configurations that are planar can therefore be described in terms of one parameter, γ, the polar equations which determine θ and ϕ, and the original set of equations.

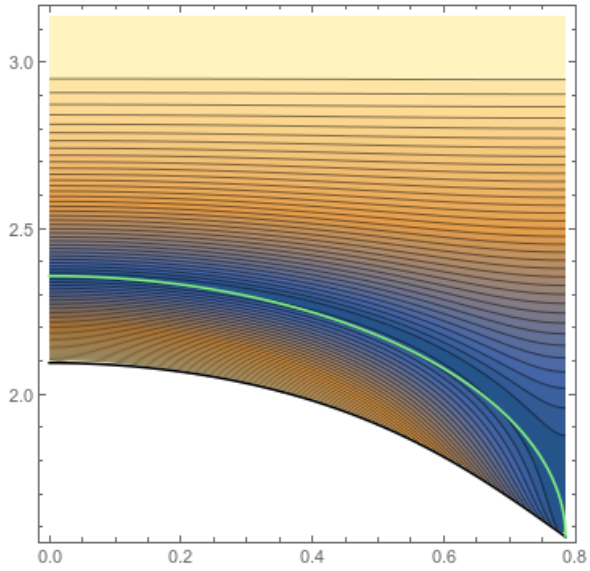

Figure 3.12: Contour plot of parallelepiped volume with the perimeter of a circle shown in green.

3.2 3D Dipolar Kagome Finite T EFM Results

3.3 3D Dipolar Kagome Magnetic Field EFM Results

In this section results on the application of an external magnetic field on the dipolar kagome lattice are presented. EFM simulations revealed how a sufficiently large external magnetic field caused the spin configuration to transition from a non-planar state to a planar state. Following this transition, the spins underwent a linear change in orientation with respect to the magnetic field magnitude by reorienting in the direction of the magnetic field. Following degaussing, the spins unaligned with the magnetic field and formed a planar state at zero magnetic field magnitude, regardless of whether the state was initially non-planar. In essence, when degaussing with a sufficiently high peak magnetic field magnitude, every minimum-energy state was transformed into a planar minimum-energy state. Finally, with sufficiently high magnetic field magnitude, the lattice became saturated and the rate at which the spins reoriented themselves along the direction of the magnetic field was reduced.

3.3.1 Magnetic Phases

The magnetization as a function of magnetic field magnitude of the 3D kagome lattice had several distinct phases of change. In figure 3.13, the magnetization lingered close to zero at low magnetic field magnitude. At some critical magnetic field magnitude, a sudden change in magnetization occured for all non-planar states after which a planar state was formed. A linear change in magnetization was observed after this critical field magnitude, until the lattice became saturated and the magnetization nearly plateaued.

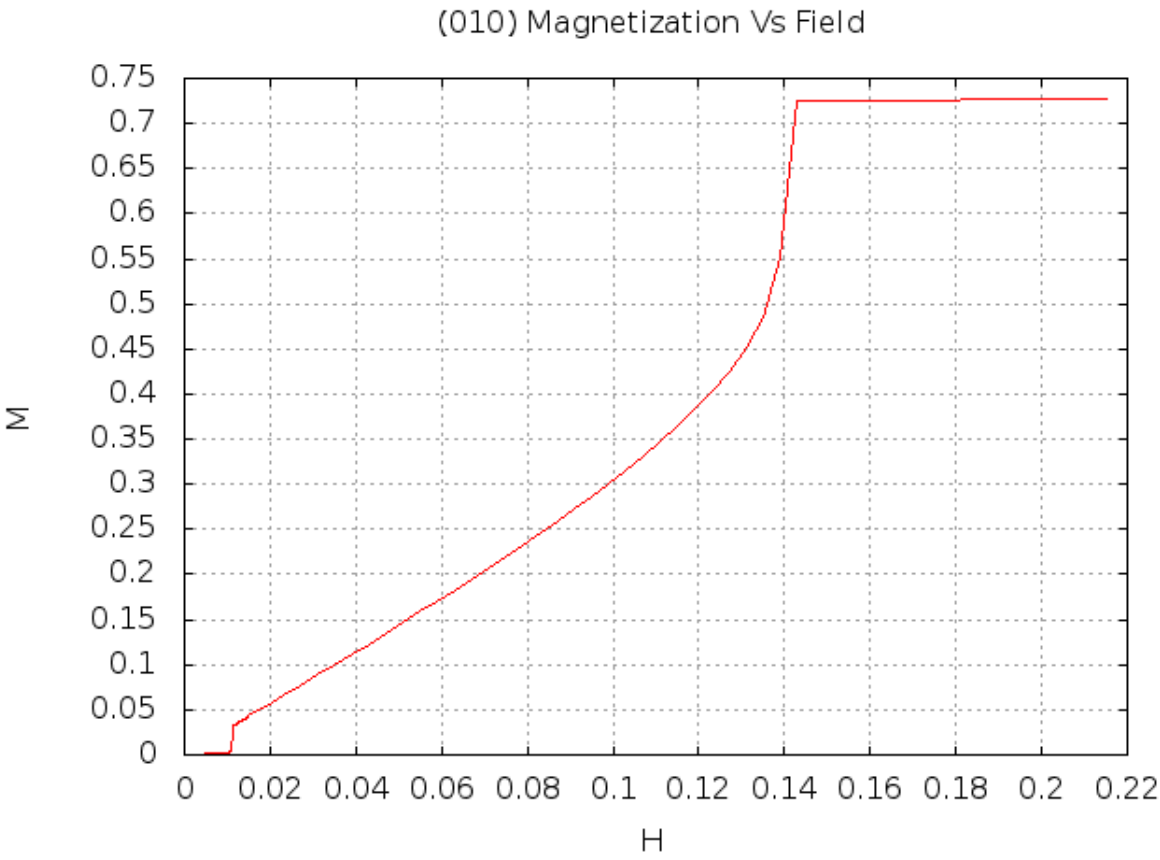

Figure 3.13: A curve of magnetization with respect to changing magnetic field magnitude of a magnetic field oriented along the y-axis.

3.3.2 Degaussing Along a Cube Axis

3.3.2.1 (001) Increasing Field

Using the state corresponding to theta=0.206275 and phi=3.11867, the effect of an magnetic field along the 001 cube axis was observed. The spin configuration begin to transition to a planar configuration at a magnetic field magniutde of 0.0105 and achieved the planar state at a magnetic field magnitude of 0.0121 as shown in fig. 3.3.2.1. The pink and brown spins swap positions, as do the blue and purple spins, as the field is increased beyond the planar state. The spins gradually align with the 001 field direction, until approximately at 0.14 the lattice becomes saturated and the red and green and spins become parallel to the field direction.

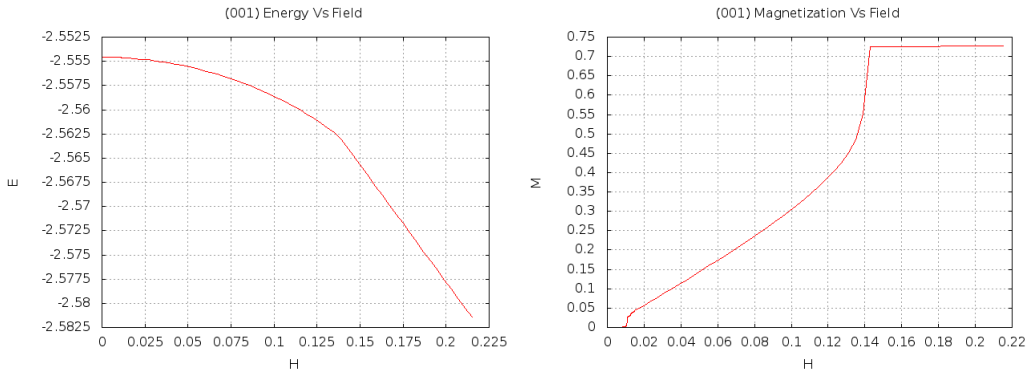

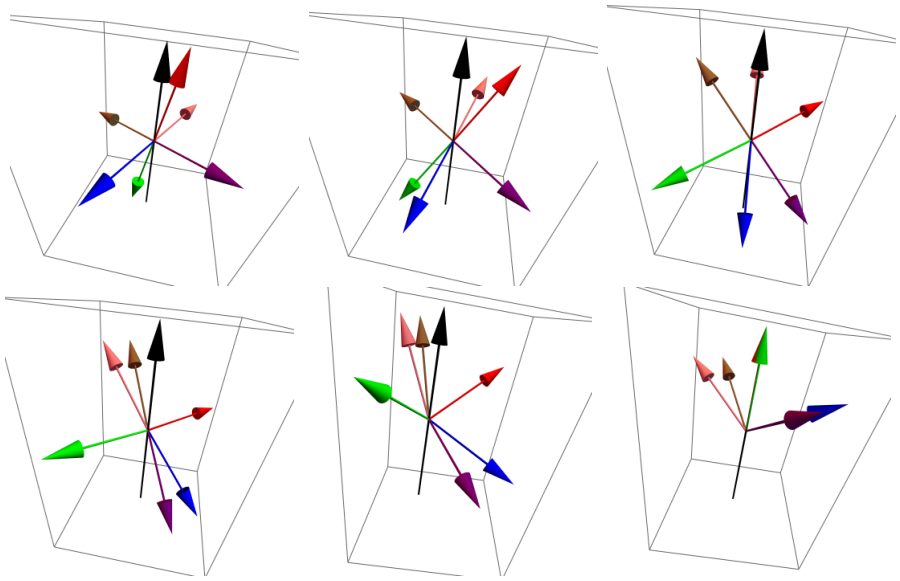

Figure 3.14: Snap shots of the 6 characteristic spins at H=0, 0.0105, 0.0121, 0.0150, 0.131, 0.151. The black arrow indicates the direction of the field.

3.3.2.2 (001) Decreasing Field

Once the lattice was saturated, the magnetic field was reduced to zero. The lattice left the saturated state at a field lower than what was required to induce it while increasing the field. The transition from saturation occured at approximately H=0.13, compared to the transition to saturation at H=0.14 when the field was decreased. The spins gradually unaligned and rested in a planar state at zero field, and was characterized by the groundstate angles theta=1.569051 and phi=0.78435097.

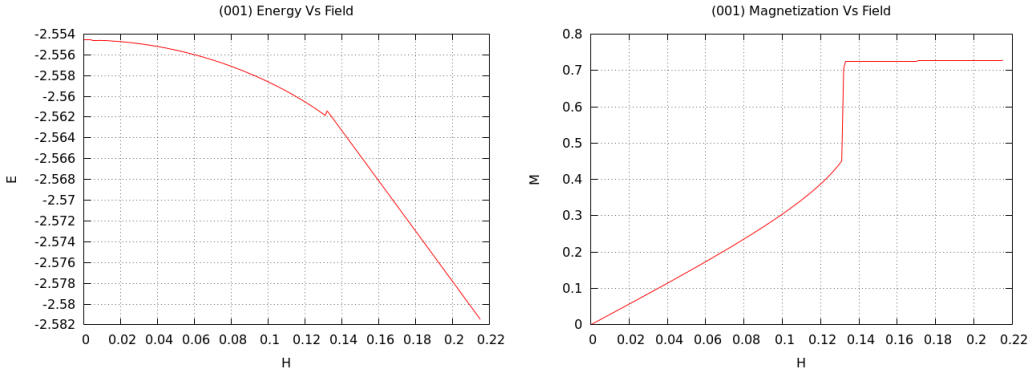

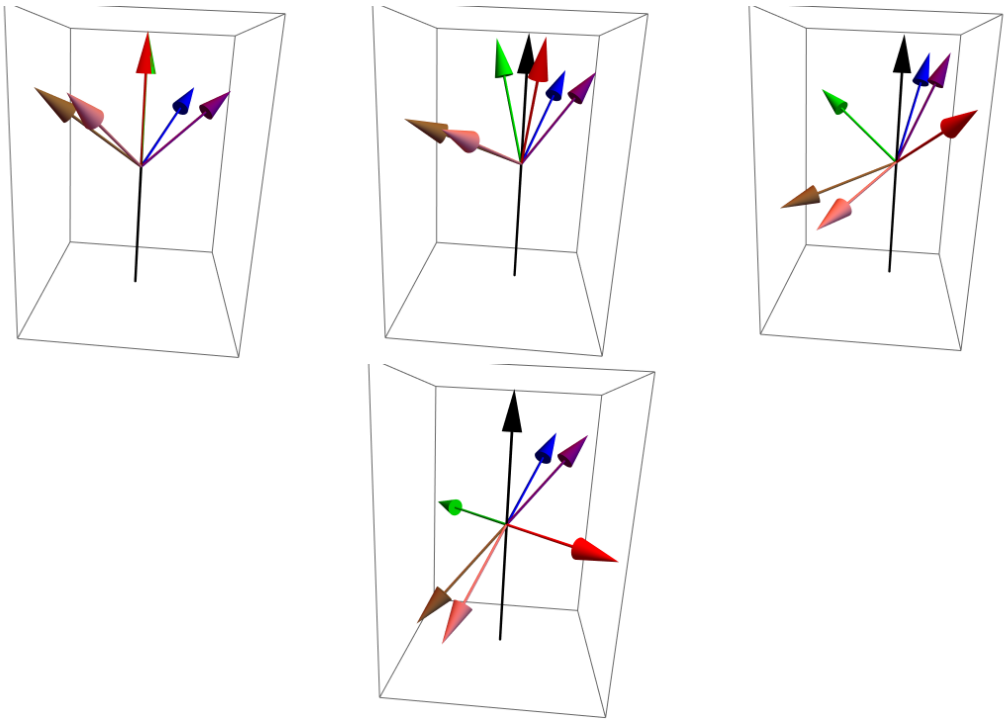

Figure 3.15: Snapshots at H=0.215, 0.132, 0.130, 0

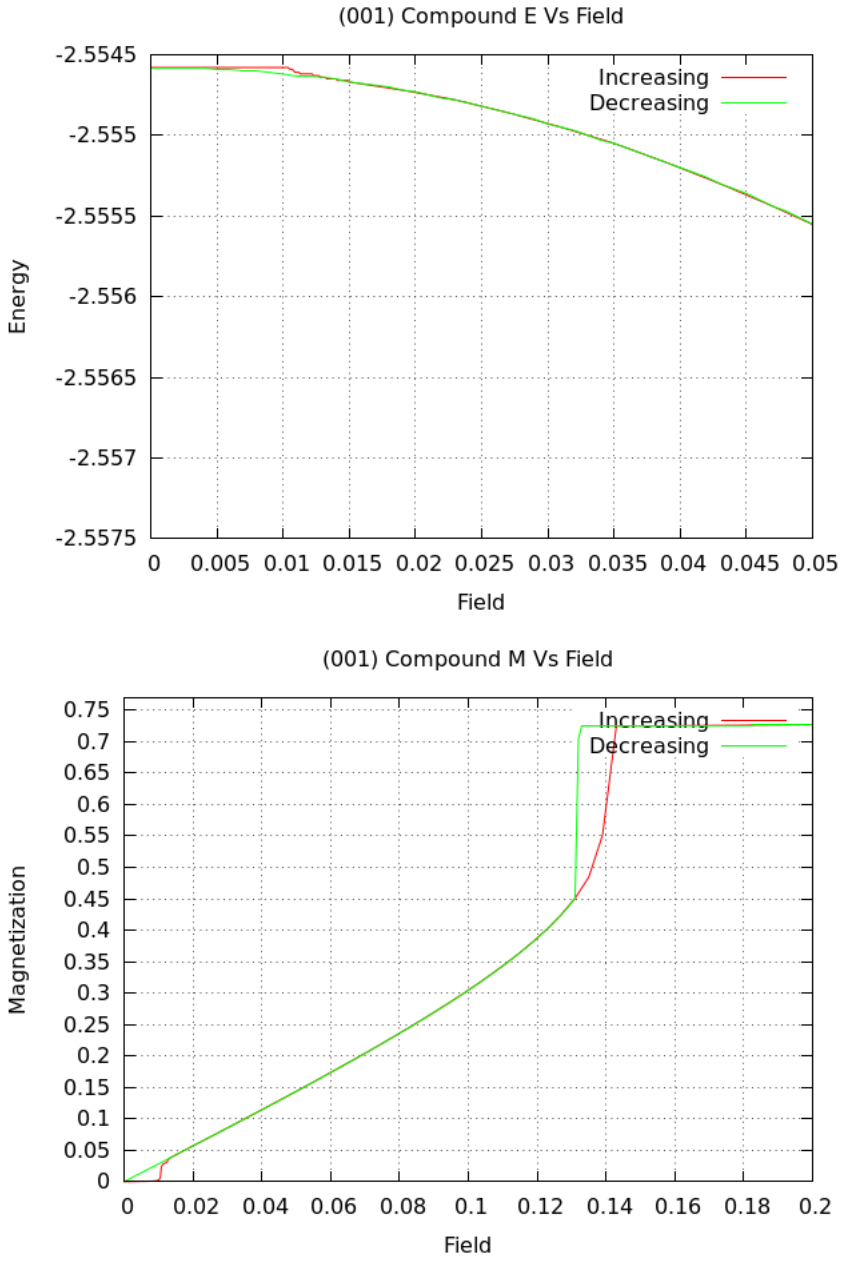

Figure 3.16: Composite graphs of energy and magnetization for both decreasing and increasing field magnitude. Note the different scales for the energy and magnetization graph. This is because plotting energy vs field on a graph which has an xrange of 0.2 reduces the ability to see any difference in the energy curves.

3.3.3 Degaussing Along a Cube Face

3.3.3.1 (011) Increasing Field

Using the state corresponding to theta=0.206275 and phi=3.11867, the effect of a magnetic field along the 011 cube face was observed. The lattice began to transition at an approximate magnetic field magnitude of 0.007. At a magnitude of 0.0074 the planar state was achieved. At 0.0093, the pink and red spins swapped position, and the blue and green spins swapped position as shown in 3.3.3.1. As the field was increased further to a magnitude of 0.0115, the green and brown spins began to swap positions. At 0.143, this interchanging of spin positions was achieved. Once saturated, no spins was parallel with the field direction.

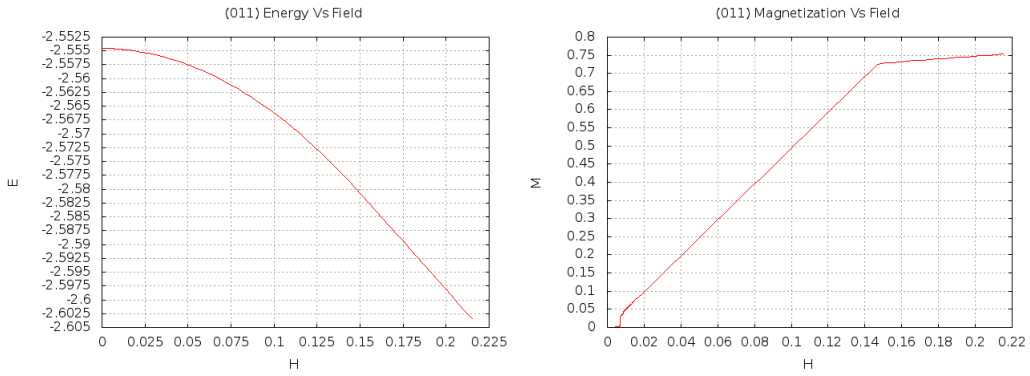

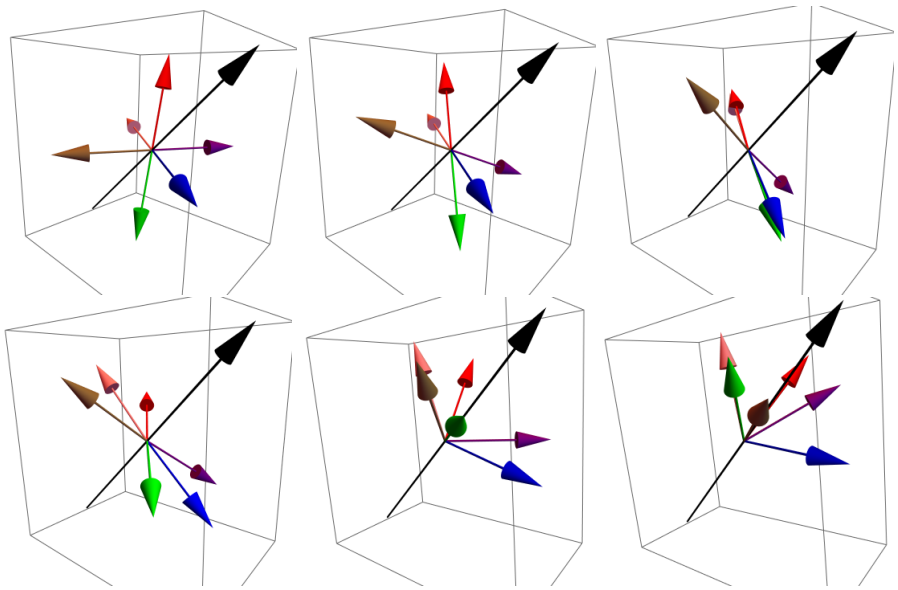

Figure 3.17: Snapshots at H=0, 0.0066, 0.0082, 0.0094, 0.115, 0.167

3.3.3.2 (011) Decreasing Field

As the field for the saturated lattice was decreased to a magnitude of 0.134, the brown and green spins swapped positions again. All 6 spins gradually unaligned with the field until they reached a zero field planar state characterized by angles theta=1.2100368 and phi=-2.428328948.

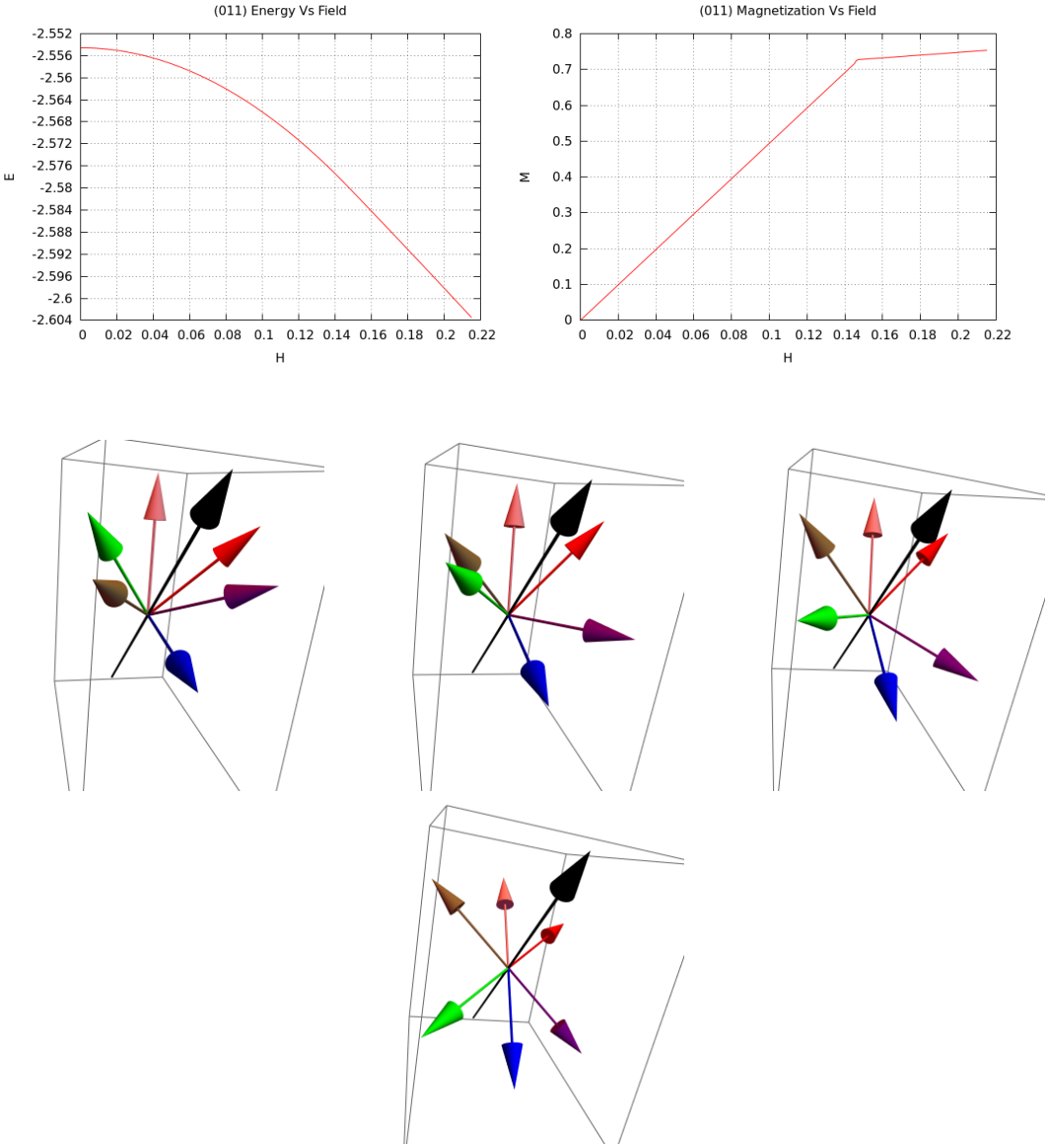

Figure 3.18: Snapshots at H=0.215, 0.134, 0.094, 0

3.3.4 Saturation of the Lattice

Using the spin configuration corresponding to theta=0.206275 and phi=3.11867, 7 simulations were run with differing field directions. The field was increased up until saturating the lattice. 001 and 010 both have identical magnetization curves, as do 011 and 101. However, 100 differs from 001 and 010, and 110 differs from 011 and 101, which is unexpected. When using the 111 field direction, saturation occurs at a field that is higher than the saturation fields of any other simulations.

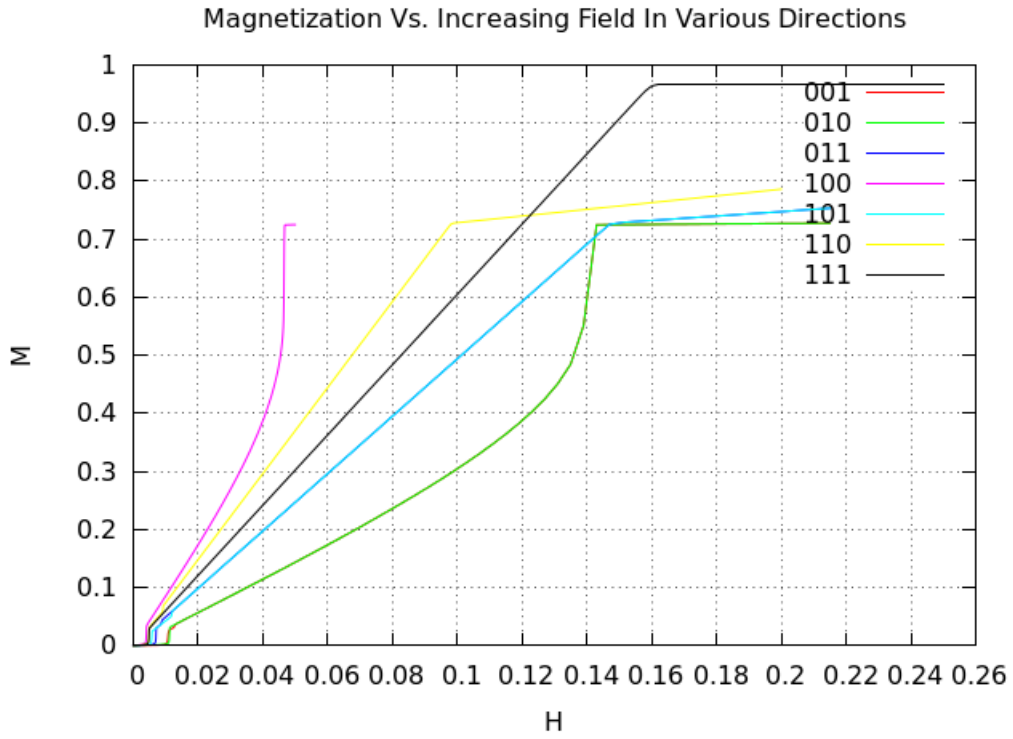

Figure 3.19: Magnetization curves starting with the same ground state and subjected to fields of various directions

3.3.5 Reduction of the Ground State Degeneracy via Application of an External Magnetic Field

The most notable result of degaussing the 3D FCC Kagome lattice with only dipolar interactions is that all possible ground states can be transformed into planar states. 26 different ground states were generated as shown in fig 3.20. Each of these states were degaussed with a field along the 111 direction.

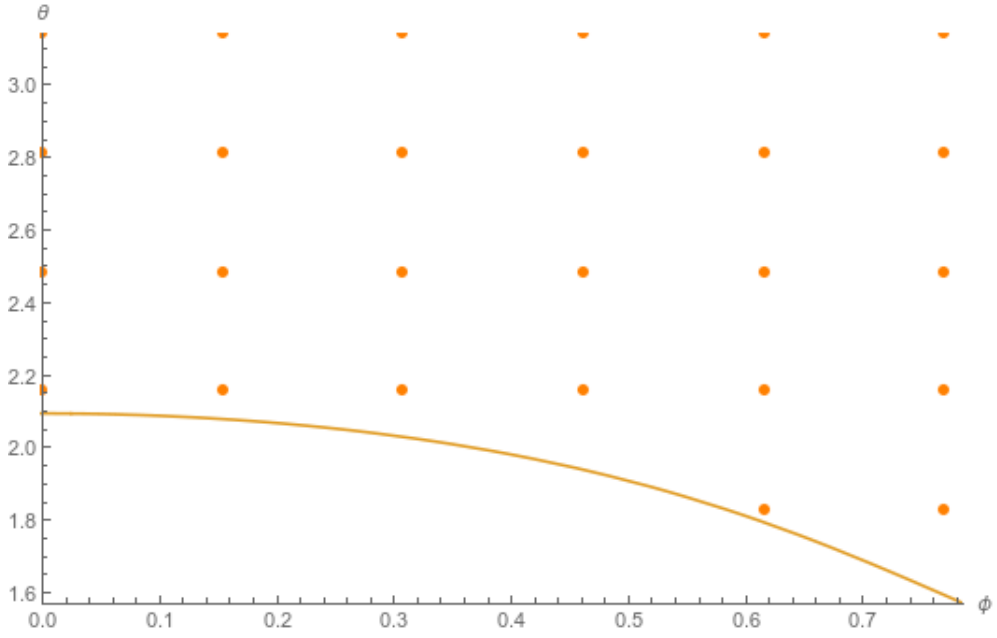

Figure 3.20: The ground state plane with an array of points selected to generate the starting states for independent degaussing simulations.

The result of these simulations is summarized in fig. 3.21. 24 of the initial states rested in the final state corresponding to theta=1.9486 and phi=0.697303, while only 2 rested in the final state corresponding to theta=1.58175 and phi=0.778825. Both of these states were planar.

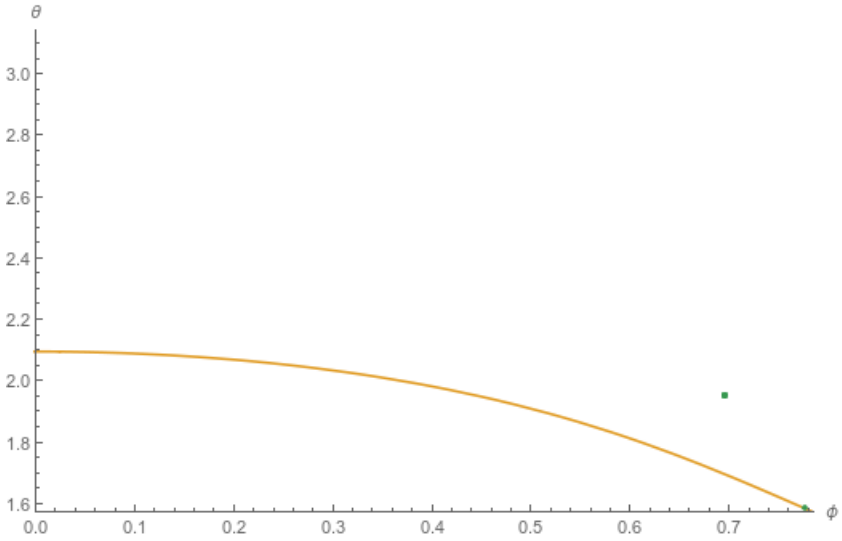

Figure 3.21: The final states following degaussing. All states are within the planar region of the plane.

Appendix A

Extra spectra

A.1 What should go in an appendix?

- raw data, extra images, extra spectra
- manuals or procedures you've written
- code
- detailed explanations of theory that don't fit in your methods chapter
- etc.